Rotator Cable Strain and the Abduction Force after Transection of the Cable Insertions

by

Christopher S. Spicer

B.S. in Mechanical Engineering, University of Pittsburgh, 2014

Submitted to the Graduate Faculty of the

Swanson School of Engineering in partial fulfillment

of the requirements for the degree of

Master of Science in Mechanical Engineering

University of Pittsburgh

2020

UNIVERSITY OF PITTSBURGH

SWANSON SCHOOL OF ENGINEERING

This thesis was presented

by

Christopher S. Spicer

It was defended on

July 16, 2020

and approved by

Mark C. Miller Ph.D., Associate Research Professor, Department of Mechanical Engineering and Materials Science

Qing-Ming Wang Ph.D., Professor, Department of Mechanical Engineering and Materials Science

Thesis Advisor: Patrick Smolinski Ph.D., Associate Professor, Department of Mechanical Engineering and Materials Science

Rotator Cable Strain and the Abduction Force after Transection of the Cable Insertions

Christopher S. Spicer, M.S.

University of Pittsburgh, 2020

The goal of this study was to assess the functionality of the rotator cable in stress-shielding the rotator crescent region. The hypothesis was that releasing the rotator cable would significantly increase strain in the rotator crescent and significantly decrease abduction force.

Surface strain and abduction force were measured for 8 cadaveric specimens for three different states of the rotator cable: intact, anterior or posterior insertion released, and both anterior and posterior insertions released. A custom-built shoulder simulator applied a physiological loading pattern to the rotator cuff muscles to simulate abduction. For each cable state, the specimen was fixed in place at both 0 and 30 degrees of abduction. Four specific regions were analyzed for strain: two areas towards the center of the rotator crescent and an area on both the supraspinatus and infraspinatus tendons. Statistical analysis was performed with anterior and posterior separated and with the two groups combined comparing the intact state to the fully released state.

No significant change was found in major principal strain across any of the four regions or two abduction angles when analyzing both the anterior and posterior groups separated and combined. A significant increase in abduction force was found at 0 degrees of abduction when the groups were combined. No other significant changes in abduction force were found.

The increase in abduction force indicates that the rotator crescent area is a better abductor than the rotator cable and is not stress-shielded by the cable. The results of the strain analysis also demonstrate this by showing no significant change upon cable release. Therefore, the rotator cable should not be relied upon to shield tears in the rotator crescent, and these tears should be surgically repaired.

Table of Contents

List of Tables

List of Figures

Preface

I would like to acknowledge the contributions of several individuals. First, I would like to thank my advisors in the lab: Dr. Christopher Schmidt, Dr. Patrick Smolinski, and Dr. Mark Miller. Secondly, I would like to thank the other graduate students I worked in the lab with: Sean Delserro, Michael Smolinski, and Ryan Blake. Thirdly, I would like to thank the fellows I worked with: Dr. Yoshiaki Tomizuka, Dr. Thomas Zink, and Dr. Dimitrios Papadopoulos. I would also like to thank the lab managers: Anthony Davidson and James Greenwell. Finally, I would like to thank my family and friends for supporting me throughout graduate school.

1.0 Introduction

1.1 Motivation

The rotator crescent was first described by Burkhart et al. as the area of the rotator cuff covering the distal insertions of the supraspinatus and infraspinatus tendons [1]. The rotator cable was described as a thick bundle of fibers bounding the crescent on its proximal side. Burkhart claimed the cable served as a suspension bridge-like stress shield for the rotator crescent and the rest of the rotator cuff. This protects these areas from tears by distributing forces away from the area. This claim is relevant due to the fact that most rotator cuff tears occur near the junction of the infraspinatus and supraspinatus, which occurs in the crescent region [2]. Knowledge of the role the rotator cable plays in load distribution could help inform how surgeons repair the rotator cuff after injury.

1.2 Goals

The goal of this project was to analyze the mechanical significance of the rotator cable in stress-shielding the rotator cuff during abduction. This study analyzed the force at the humerus and the strain in the rotator cuff during abduction, specifically focusing on the rotator crescent area and the rotator cable.

2.0 Background

2.1 Anatomic Definitions

Given that the human body has various possible orientations, a standard anatomical position for humans has been defined, shown in Figure 1. Several terms are used to define locations on the body relative to this position. Superior and inferior mean closer and further from the head, respectively. Anterior and posterior refer to front and back, respectively. Medial means closer to the vertical midline of the body, lateral means further from the midline. Internal rotation refers to rotation toward the midline, and external rotation refers to rotation further away from the midline. Distal and proximal refer to location relative to extremities: distal being further away from the trunk, and proximal being closer.

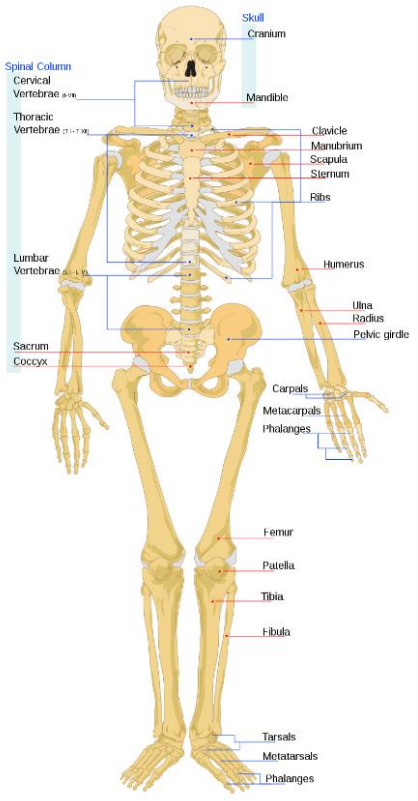

Figure 1. Standard Anatomic Position (en.wikipedia.org)

2.2 Shoulder Anatomy

The focus of this research is the tissues of the rotator cuff, which are located in the shoulder. The shoulder joint is made up of the humerus and the scapula bones, where the humerus articulates in the socket of the scapula (glenoid). Upper extremity skeletal anatomy is shown in Figure 2. This joint is known as a ball-and-socket joint, which allows for a wide range of motion.

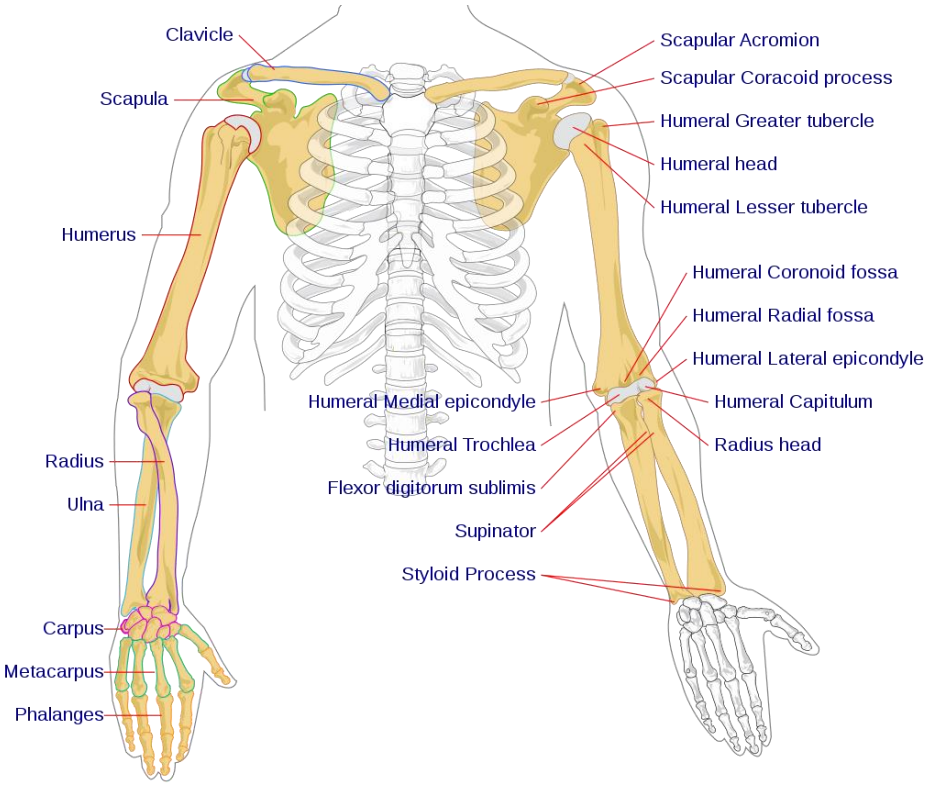

Figure 2. Skeletal Anatomy of the Shoulder (en.wikipedia.org)

An illustration of the muscular anatomy of the shoulder is shown in Figure 3. This set of muscles control the movements of the shoulder. Flexion is controlled by the pectoralis major, the biceps, and anterior deltoid. Extension is controlled by the posterior deltoid, latissimus dorsi and teres major. Abduction is controlled by the middle deltoid and supraspinatus. Internal rotation is

provided by the subscapularis, pectoralis major, latissimus dorsi, teres minor and anterior deltoid. External rotation is controlled by the infraspinatus and teres minor. The overall stability of the joint is managed by a group of four muscles (teres minor, infraspinatus, supraspinatus and subscapularis) that make up a structure known as the rotator cuff.

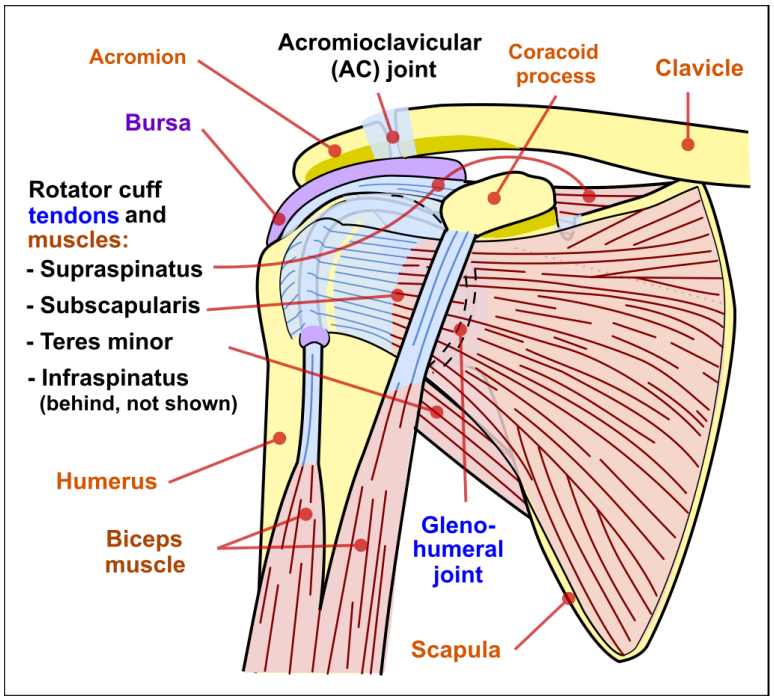

Figure 3. Muscular Anatomy of the Shoulder (en.wikipedia.org)

2.3 Rotator Cuff Anatomy

The rotator cuff is made up of four muscles (listed posterior to anterior): the teres minor, infraspinatus, supraspinatus, and subscapularis. Each muscle is defined with an origination point and an insertion point, and all muscles are oriented from medial to lateral. The teres minor originates on the upper two-thirds of the lateral border of the scapula and inserts below the

interior facet of the greater tubercle of the humerus. The infraspinatus originates on the fossa of the scapula and inserts at the posterior aspect of the greater tuberosity of the humerus and the capsule of the shoulder joint. The supraspinatus originates at the supraspinatus fossa and inserts on the greater tuberosity of the humerus at the superior facet. The subscapularis originates at the subscapular fossa on the anterior surface of the scapula and inserts into the lateral tuberosity of the humerus and the front of the shoulder joint capsule.

The region near the supraspinatus and infraspinatus tendons of the rotator cuff is broken up into five layers [3]. The first layer is made up of the fibers of the coracohumeral ligament (CHL). The second layer is made up of the parallel fibers of the supraspinatus and infraspinatus tendons. Layer three is a thick cross-hatched tendinous structure. The fourth layer is made up of collagen fibers, and is known as the rotator cable. Layer five is known as the capsule, which serves as a thin sheath around the humeral head, attaching laterally at the neck of the humerus and medially on the glenoid and labrum.

The aforementioned rotator cable was first described by Burkhart et al in an anatomical study [1]. In this study, Burkhart proposed that the cable was mechanically significant, stress-shielding the rest of the crescent area. Burkhart et al likened the cable to a suspension bridge in this way (Figure 4), making tears in the area in the cuff directly inferior to the cable (crescent area) biomechanically insignificant.

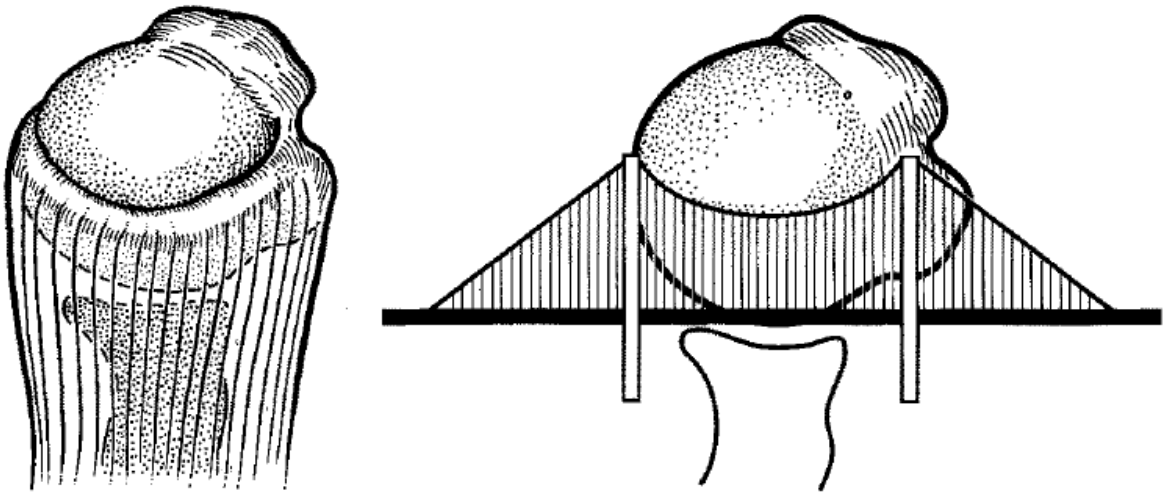

Figure 4. Illustration comparing rotator cable to suspension bridge [1]

2.4 Injuries of the Rotator Cuff

As a central structure in upper extremity function, the rotator cuff can be susceptible to injury, specifically tears. Much of the time, these tears are not mechanically relevant enough to be impactful, and therefore do not require surgery [4,5]. Tears that cause loss of mechanical function (often instability) or cause pain in the individual are impactful enough to require surgery. Some tears of the cuff, known as massive tears, cannot be surgically repaired. Often times they are irreparable due to tendon retraction with muscle atrophy, fatty infiltration and inelasticity.

2.5 Previous Strain Methodologies

Previous biomechanical studies have used various methods to asses strain. In an early experiment by Renström et al, a Hall effect strain transducer (HEST) was used to measure strain in the anterior cruciate ligament (ACL) during hamstring activity, quadriceps activity and combined activity of the two (Figure 5) [6]. The study concluded that independent hamstring activity decreased ACL strain. A later test performed by Reilly et al used a differential variable reluctance transducer (DVRT) to calculate strains of supraspinatus tendon in vitro on both bursal and articular sides [7]. The study found that strain was significantly different between the bursal and articular sides during both static loading and abduction. A similar study was performed by Mazzocca et all to determine the effect of partial-thickness tears on the supraspinatus tendon [8]. The study concluded that the tendon strain on the articular side increased significantly with simulated tears of increasing size. HESTs work using a magnet and measuring the voltage output proportional to the strength and therefore change in relative distance to the magnetic field. DVRTs also use a magnetic field but instead achieve this field with a coiled wire. Both HEST and DVRT involve the attachment of a strain gauge to the specimen.

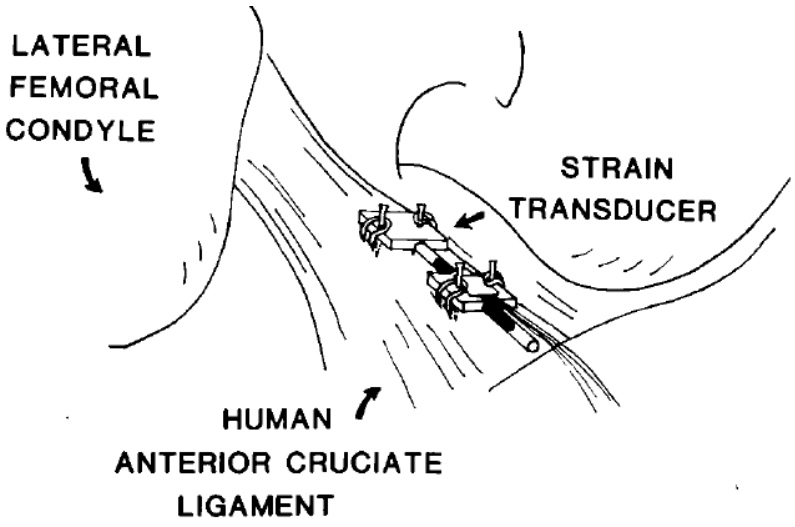

Figure 5. An HEST measuring strain in the ACL [6]

A study published in 2008 documented the use of a digital image correlation (DIC) system to measure strain on sheep tendons. This study found correlation between tear size and magnitude of the strain [9]. DIC does not use a strain gauge and instead involves a random speckle pattern painted on the surface of a specimen. DIC does not affect the specimen mechanically, giving it an advantage over other strain methods. HEST and DVRT both need to be attached to the specimen, potentially altering the mechanical properties and overall strain. DIC also has an advantage over strain transducers in its ability to capture multi-directional strain over an area. HEST and DVRT measure strain in one fixed dimension, while DIC measures strain over areas in two dimensions. This allows for major and minor principal strains to be found, as well as their directions.

2.6 Previous Rotator Cuff Strain Studies

A study published in 2002 used magnetic resonance imaging (MRI) to measure strain in the rotator cuff [10]. Strain was measured in the supraspinatus tendon using measurements on the MRI at three locations (superior, middle, inferior) and four abduction angles (15, 30, 45 and 60°), shown in Figure 6. The study concluded that strain was consistent across different regions of the supraspinatus and the position of the humerus in the glenoid played a large role in the overall mechanics of the rotator cuff.

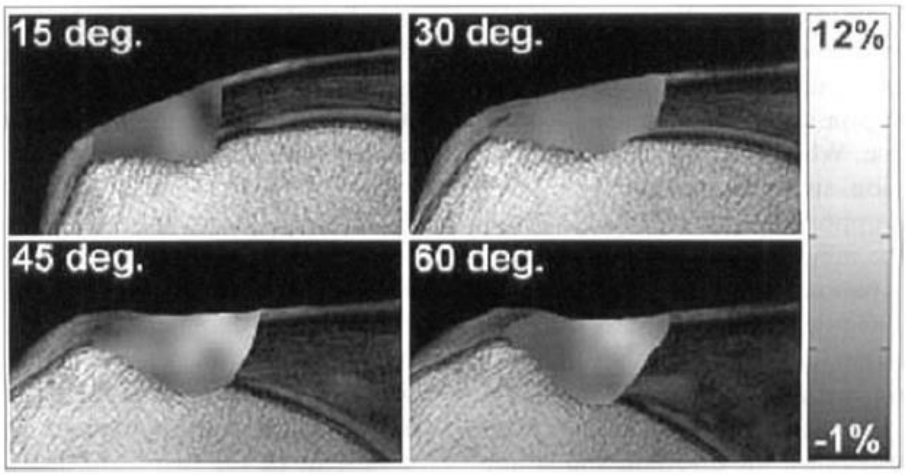

Figure 6. MRI of the supraspinatus tendon at four different abduction angles [10]

A recent study measured strain in the rotator cuff using a set of fixed strain markers shown in Figure 7 [11]. This study analyzed the effect of a supraspinatus tear on the distribution of strain and the propagation of the tear during cyclic loading. It was found that the strain shifted with tear propagation and that the tear propagation remained isolated to the tendon. Another study by the same lab used finite-element modeling and simulation to analyze strain around supraspinatus tears and concluded that anterior tears were more likely to propagate [12].

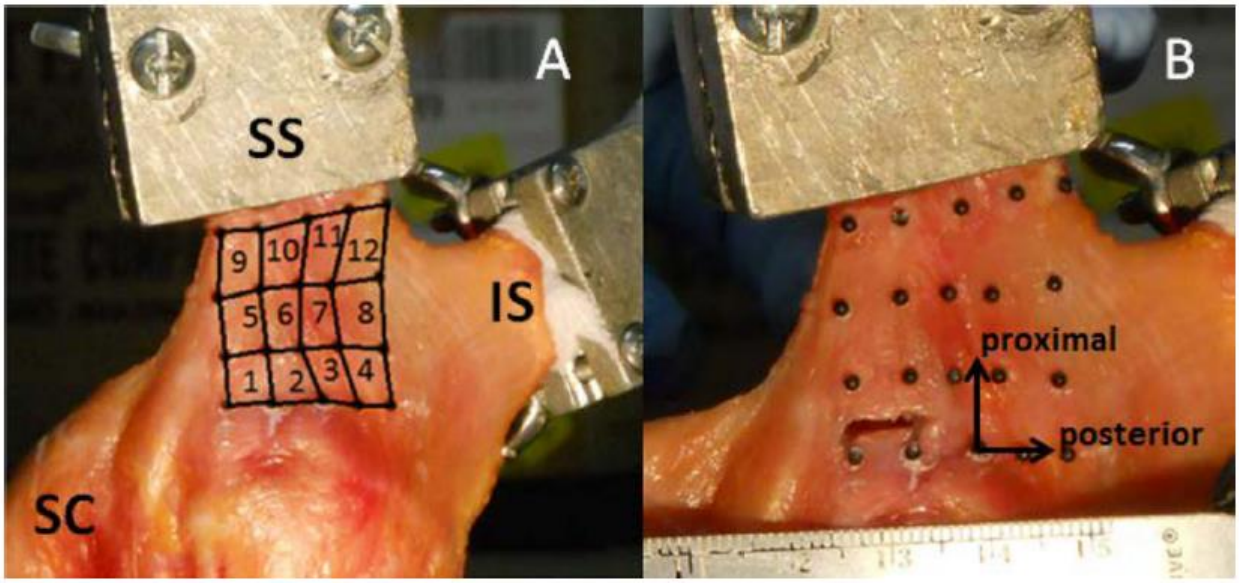

Figure 7. Strain markers on the rotator cuff [11]

2.7 Previous Rotator Cuff Reaction Force Studies

Other studies examined stability in the glenohumeral joint in relation to the rotator cable. A study by Pinkowsky et al. examined the effect of releasing the rotator cable on shoulder stability. An anterior load was applied to the humerus and glenohumeral translation was measured at 30, 60, 90 and 120 degrees of external rotation. The study determined that tears with a thickness greater than 50% involving the cable increased glenohumeral translation [13]. Another study examined strain, tear progression and tendon stiffness in relation to the release of the cable. This was achieved by clamping the rotator cuff muscles and cyclically loading the supraspinatus. The study concluded that tears that involved both the cable and the crescent had higher strain, higher gap formation and lower tendon stiffness than tears in just the crescent [14]. Another study examined the effect of different loading ratios on glenohumeral abduction. This study found consistent abduction between trials when the same loading ratio was used, but did

not determine an ideal loading ratio to simulate abduction [15]. A 2002 study examined the reaction forces at the glenohumeral joint when the supraspinatus and infraspinatus were torn. The study found that tears in the supraspinatus did not have a significant effect on the resulting forces, but tears stretching more anteriorly and posteriorly had a significant change on the magnitude and direction of the resulting forces [16].

3.0 Methods

3.1 Overview

The goal of this study was to determine the mechanical relevance of the rotator cable in regards to shoulder abduction by applying a physiological load to the rotator cuff muscles while measuring strain and humeral abduction force.

Eight cadaveric shoulder specimens were mounted and fixed in a custom-built shoulder simulator. The simulator consisted of a proportional-integral feedback control system with five actuators and a pulley system to apply loads in physiological directions. These loads were applied to the individual rotator cuff muscles while strain on the surface of the rotator cuff and abduction force at the humeral end were recorded. This testing was performed with the humerus fixed at both 0° and 30° of abduction. The cable's anterior or posterior insertions were released, and the tests were repeated. The cable was then fully released by cutting the opposing insertion site, and the final tests were performed.

Statistical analysis was performed using a one-factor repeated measures ANOVA, and if the ANOVA was significant, followed by post-hoc Bonferroni correction for the abduction forces and strain regions of interest to determine if the release of the rotator cable had any mechanical effect.

3.2 Shoulder Simulator

Mechanical loading and fixture of cadaveric specimens was achieved using a custom shoulder simulator shown in Figure 8. Five actuators applied muscle loads with wires, and

physiological force lines of action were achieved by routing the wires through a system of pulleys and attaching them to sutures sewn into the muscles of the specimens. Feedback control was achieved by attaching a single degree-of-freedom load cell (MLP-100, Transducer Techniques, Inc.) to each actuator. A large arc centered vertically at the front of the simulator allowed the humerus to be set at different angles of abduction.

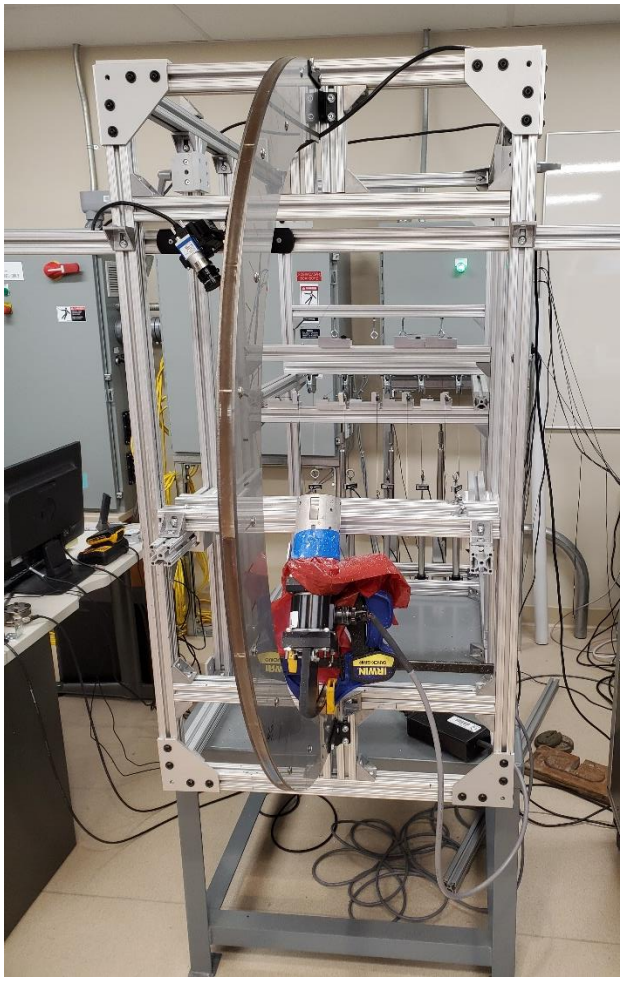

Figure 8. The simulator used for testing

3.3 Data Acquisition

Loading of the cadaveric specimens in the shoulder simulator was achieved using a proportional-integral controller (DMC-4080, Galil Motion Control). Single degree-of-freedom load cells were connected to signal conditioners (LCA-RTC, Transducer Techniques) which provided the control system with the load being applied by the actuator. This allowed the proportional integral control to continuously calculate the error signal between the input loads and the actual loads and adjust the servo drives (Compax3, Parker Hannifin Corp.) for each actuator accordingly.

Abduction force was measured using a six degree-of-freedom load cell that was fixed between the arc of the simulator and the humerus of the cadaveric specimens. The output of this load cell was connected to an external digital-to-analog converter and fixed gain analog amplifier (AM6501, Bertec Corp.) and then to a data acquisition board (NI USB-6008, National Instruments, Inc.). This data acquisition board was connected to the control system computer to store the data output files.

A Digital Image Correlation (DIC) system (Vic-3D, Correlated Solutions) was used to measure the strain on the surface of the rotator cuff. DIC is an optical tracking system which takes a series of images of a specimen undergoing a deformation and uses those images to measure the strain on the surface of the specimen. The system accomplishes this using a contrasting speckle pattern applied to the specimens, splitting this pattern into smaller areas known as subsets, and tracking how each of the subsets move and deform.

To take these images, two cameras were mounted to the simulator and were positioned so that the surface of the rotator cuff near the cable was in view. Prior to testing, the system was

calibrated by capturing a series of images (Vic-Snap, Correlated Solutions) of a calibration plate (5mm, Correlated Solutions) and processing the images using Vic-3D.

3.4 Cadaveric Specimen Preparation

Eight fresh-frozen human cadaveric shoulder specimens with no rotator cuff pathology were used in this study. Prior approval was obtained from the University's Committee for Oversight of Research and Clinical Training Involving Decedents (CORID #1012). Specimens were thawed to room temperature. The distal humerus was removed below midshaft, and soft tissues were removed leaving the rotator cuff and the shoulder capsule intact. The medial half of the humeral head was removed in order to mark the outside of the rotator cable with black suture (Figure 9). This was done because the fibers of the cable are visible from the inferior side, but not the bursal. The humeral head was then reattached using a screw. Krakow stiches were sewn in each of the rotator cuff muscles, dividing the subscapularis into an upper and lower section. Eyelet screws were attached into the scapula to give anatomic lines of action to the sutures. The scapula was secured into a custom-built aluminum box using polyester resin (Bondo, 3M), and the humeral head was similarly secured into a section of PVC pipe.

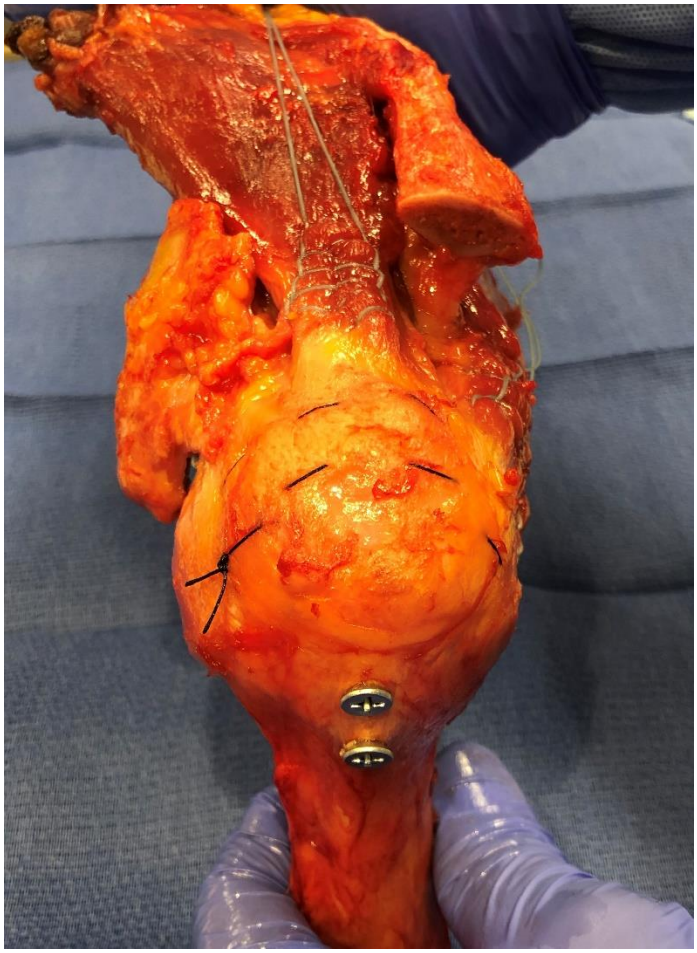

Figure 9. A specimen with its rotator cable stitched

3.5 Test Protocol

The aluminum scapula box was positioned on the custom-built shoulder simulator with the joint centered in the arc, and the humeral shaft was fixed at 0 degrees of abduction. The sutures on the rotator cuff muscles were attached to the cables of the actuators. A speckle pattern was applied to the surface of the rotator cuff by first staining the specimens with a methylene blue solution and then speckling the specimens with waterproof white ink, using a toothbrush to spray a random pattern (Figure 10). The cameras were then positioned above the specimen to

capture the strain pattern on the bursal side of the cuff. A pre-load of 5N was applied to all of the rotator cuff muscles. Once the pre-load was applied, static physiologic loads emulating abduction (Table 1) were then applied to the rotator cuff muscles for one minute. The muscle loads were calculated using published data on physiological cross-sectional area and electromyography activity [15]. The separation of the subscapularis loads into upper and lower was achieved using existing data on measured sugar intake during activity using positron emission tomography [17].

Figure 10. A specimen stained with dye and speckled with paint

Table 1. Muscle Loads Used for Testing

Muscle	Lower Subscapularis	Upper Subcapularis	Supraspinatus	Infraspinatus	Teres Minor
Load (N)	127	108	80	90	97

During the test, strain was measured using a DIC (Digital Image Correlation) system and the resulting humeral abduction force was measured at the distal humerus using a six degree of freedom force sensor. After the specimen was tested with the cable intact, the rotator cable was released (Figure 11) at either the anterior or posterior end. Randomization of which insertion was released first was determined with a random number generator. The previous testing steps were then repeated at 0 and 30 degrees of abduction for the single-release specimen. The opposite insertion of the cable was then released, and the test procedure was again repeated for 0 and 30 degrees of abduction.

Figure 11. A specimen with an incision made for cable release (incision circled)

3.6 Data Analysis

The forces at the distal humeral end of the specimens for every test were determined from output values in the direction of interest from the 6-DOF load cell. The abduction force was defined as the force on the axis perpendicular to the midline of the humerus pointing directly in the medial direction. The forces were continuously recorded throughout the test, so total abduction force was found by subtracting the abduction force before loading from the abduction force after loaded.

To calculate the strain, the DIC system required an overall region of interest to be drawn over the initial image in the set of images (Figure 12). This region needed to be selected to be used for the two specimen abduction positions, so the region was drawn to include the crescent area, the cable, and the tendinous insertions to the cable, specifically around the supraspinatus and infraspinatus. An image was taken of the specimen before the stain and speckle were applied to use as reference for the cable location.

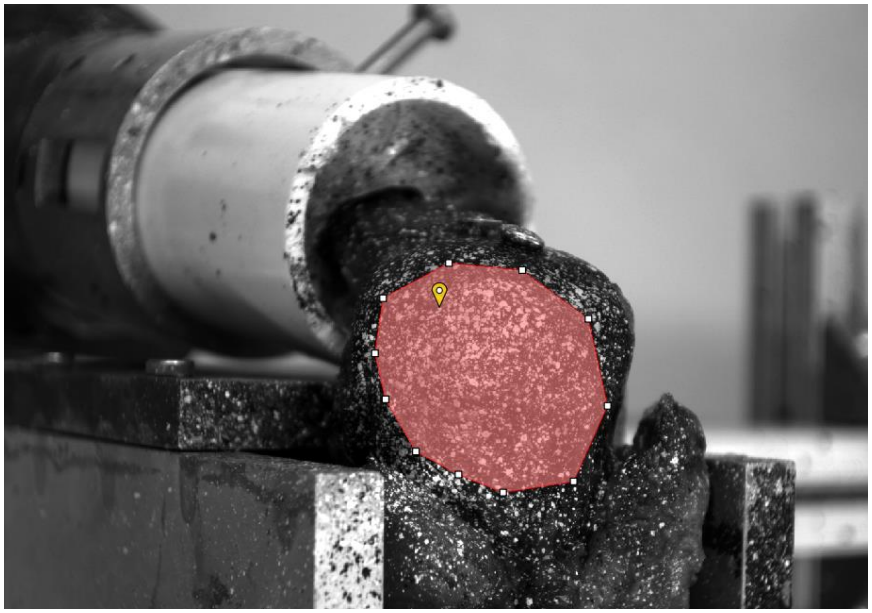

Figure 12. The region of interest over which strain was calculated

Four smaller regions of interest were identified on each specimen, shown in Figure 13. The first regions, labeled A and B on the figure, were in the crescent area within the rotator cable. To help with standardization of regions A and B, a line was drawn down the middle of the supraspinatus tendon and the sutured cable was used (highlighted in blue on the figure). The length of this line between the two sides of the cable was used to select regions A and B. Measuring from the top section of the cable, the center of region A was one full cable length away, and the center of region B was one half of a cable width away. The third and fourth regions, labeled C and D, were just outside the rotator cable on the infraspinatus and supraspinatus, respectively. All four of the regions were on tendon as opposed to muscle to ensure the measured strain was on the cuff itself as opposed to the surrounding muscles.

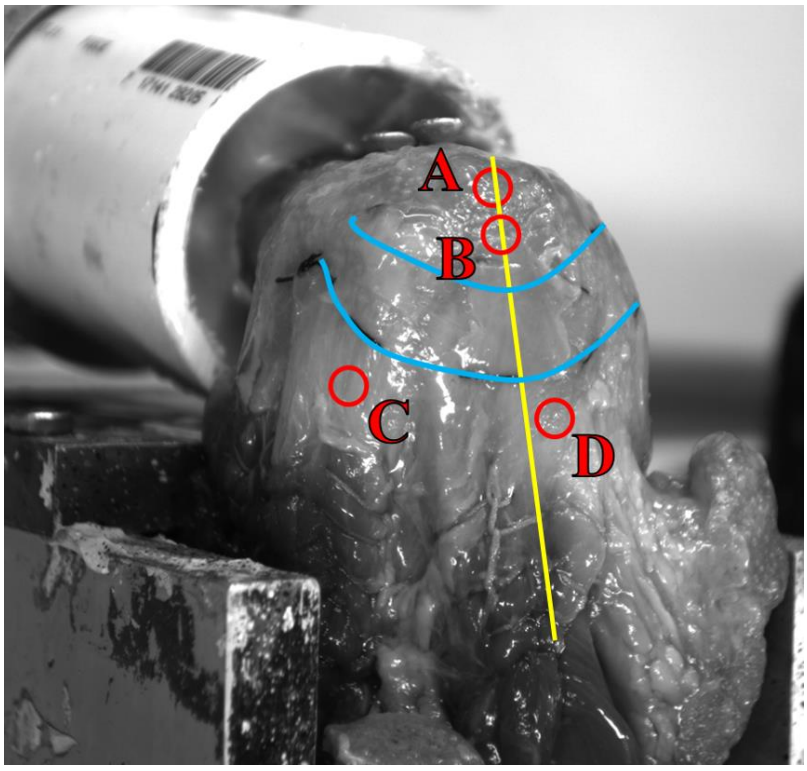

Figure 13. Specific regions strain was observed

The strains in the identified regions of interest were found by using the “inspect” tool in the DIC software to find the average strain within a circle (Figure 14). The sizes of the circles were measured using pixel measurements given from the program, and those pixel measurements were converted to mm using the calibration output from the software. A standardization of 4mm in diameter was used for each circle.

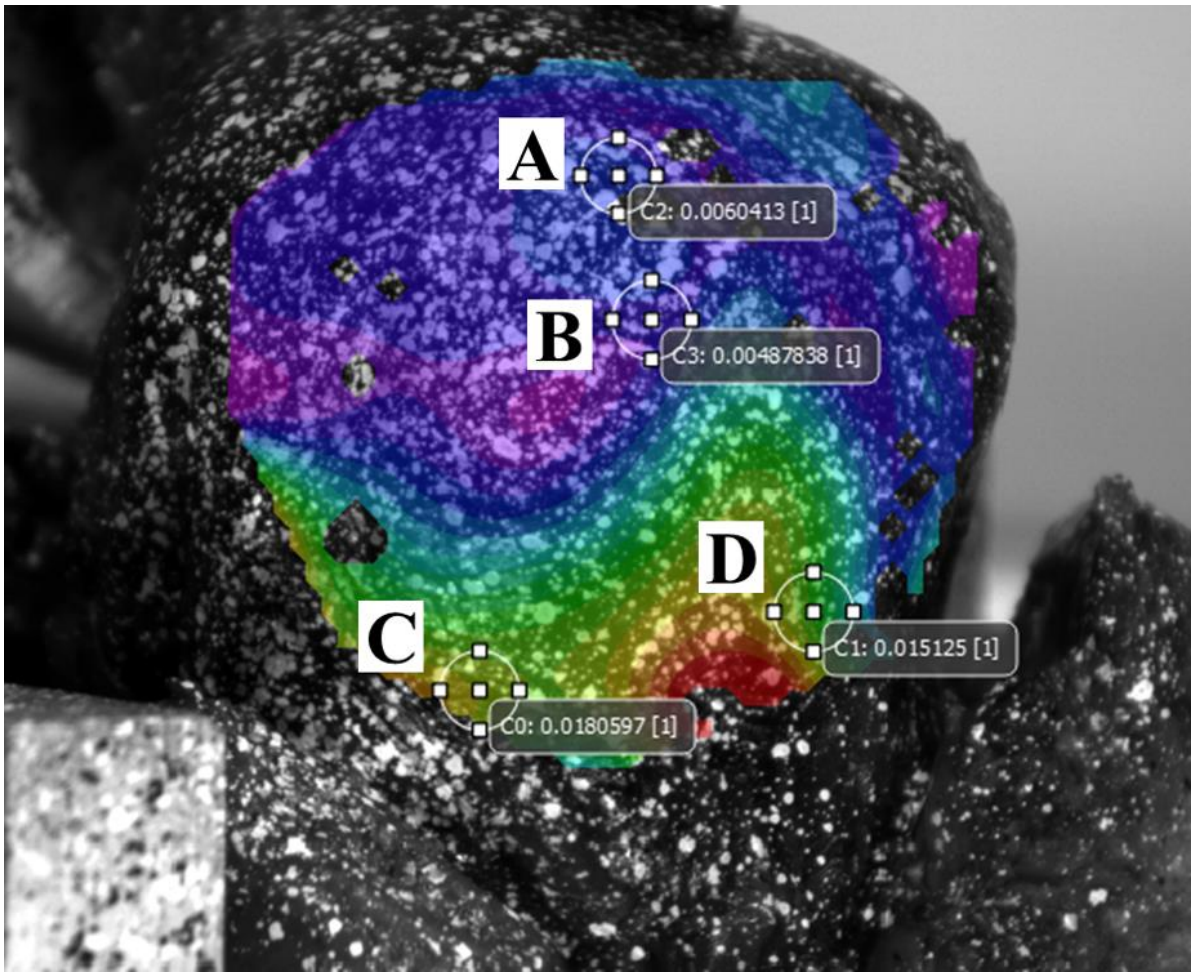

Figure 14. Strain plot with circular regions of interest

The DIC software reported directional strains based on a coordinate system, shear strain based on these coordinates, major principle strain and minor principal strain. The major principle strain, referred to as “e1,” was chosen for analysis.

3.7 Statistical Analysis

The data for the specimens was separated into an anterior release first group and a posterior release first group, with four specimens in each group. The data for the 0 and 30 degree abduction angles was analyzed separately within these groups. Statistical comparisons for abduction force and the four strain regions of interest were performed in each group by comparing both the single release and the full release values to the native. Statistical analysis was performed using a one-factor repeated measures analysis of variance (ANOVA) with the cable state as the factor, followed by post hoc analysis using a Bonferonni correction with statistical significance at $p<0.05$ (SPSS, IBM) if the ANOVA showed significance.

4.0 Results

4.1 Abduction Force Results

Anterior and posterior abduction force results are shown in Figure 15. Single release is referred to as "1Cut," and full release is referred to as "2Cut." No significant differences were found in either the anterior or posterior groups, with the smallest p-value being 0.062 between the intact and full release states at 0 degrees in the anterior release group. Combined abduction force results are shown in Figure 16. Significance was found at zero degrees of abduction between the intact and released groups with a p-value of 0.003.

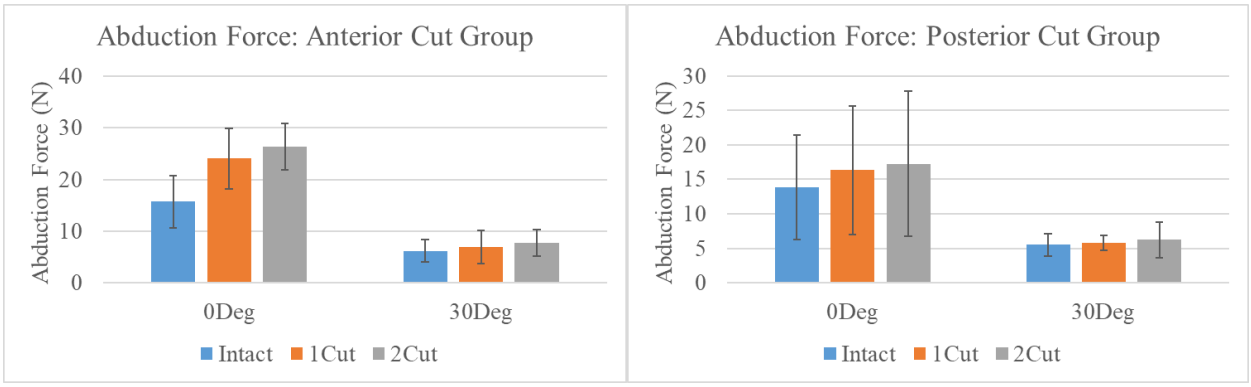

Figure 15. Anterior and Posterior Groups Abduction Force Results

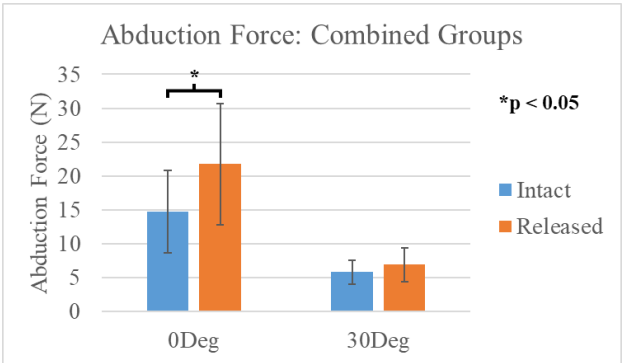

Figure 16. Combined Anterior and Posterior Group Abduction Force Results

4.2 Strain Results

Anterior and posterior strain results in four different locations are shown in Figures 17-20. Major principal strain was used for analysis, referred to in the graphs as "e1." No significant differences were found in either the anterior or posterior groups at any of the strain locations, with the smallest p-value being 0.250 in the infraspinatus between the intact and single release states at 0 degrees in the anterior release group. Combined strain results are shown in Figures 21-24. No significant differences were found at any of the strain locations, with the smallest p-value being 0.237 at the medial crescent between the intact and full release states at 0 degrees.

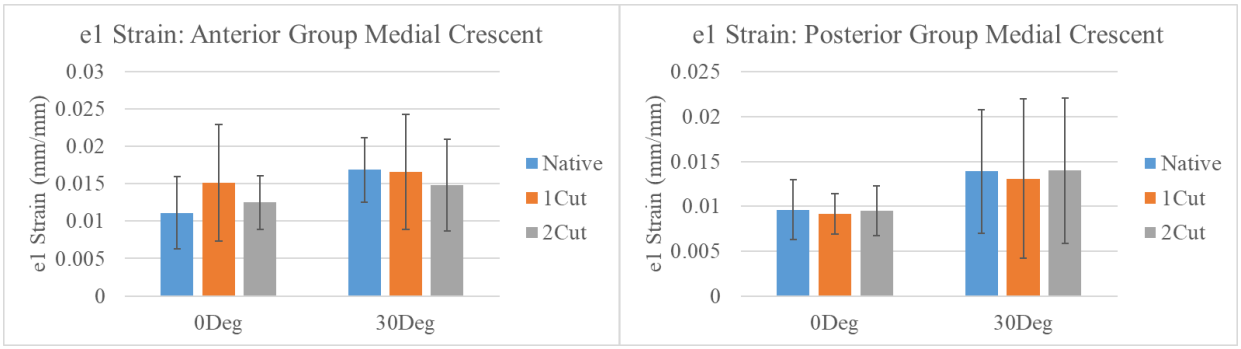

Figure 17. Anterior and Posterior Groups Medial Crescent Strain Results

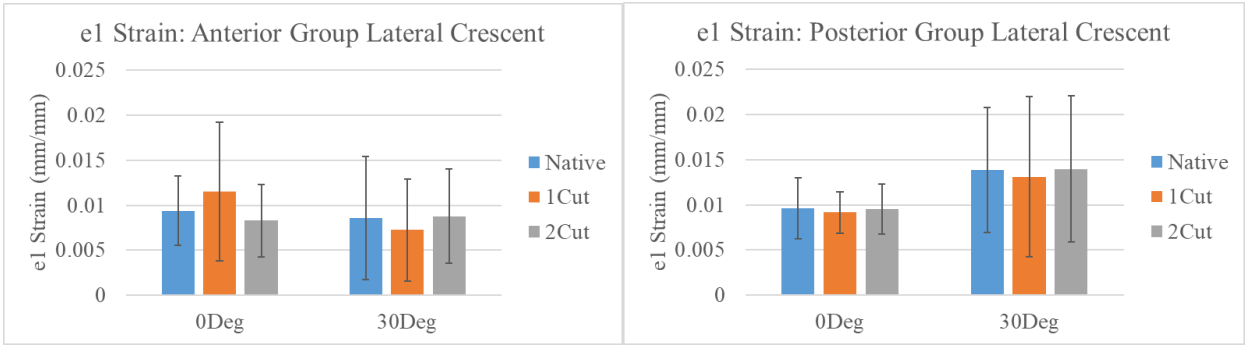

Figure 18. Anterior and Posterior Groups Lateral Crescent Strain Results

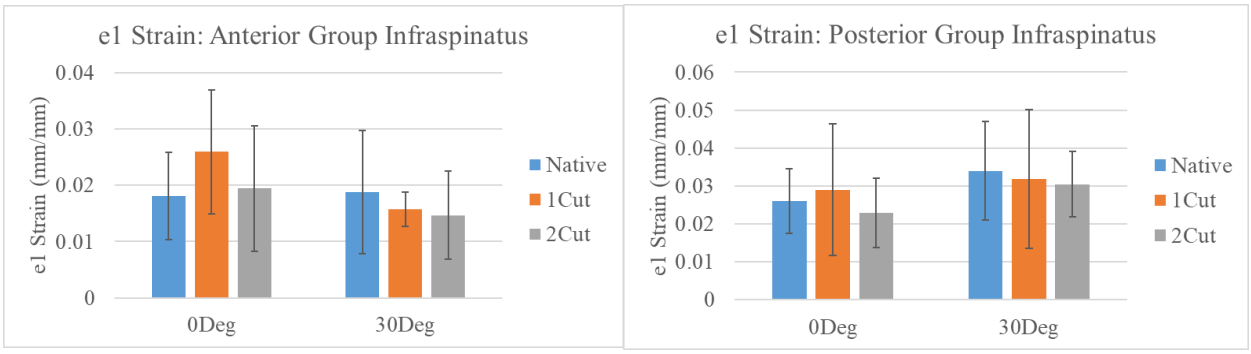

Figure 19. Anterior and Posterior Groups Infraspinatus Strain Results

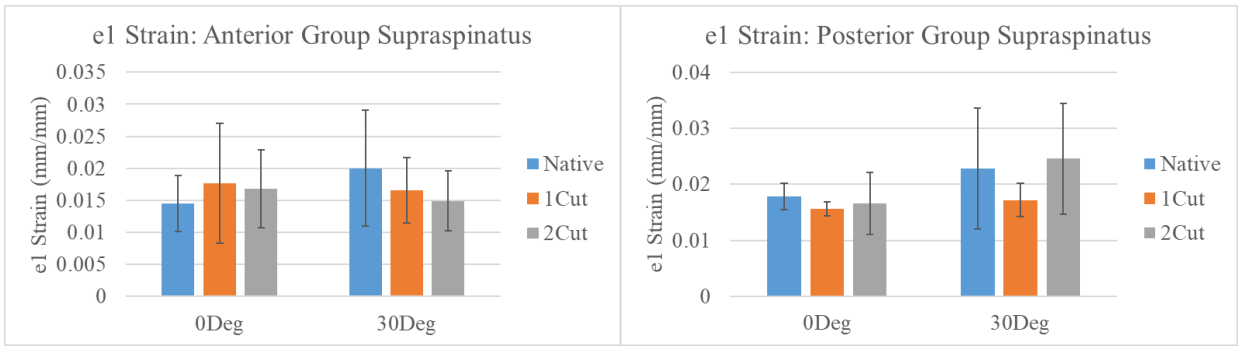

Figure 20. Anterior and Posterior Groups Supraspinatus Strain Results

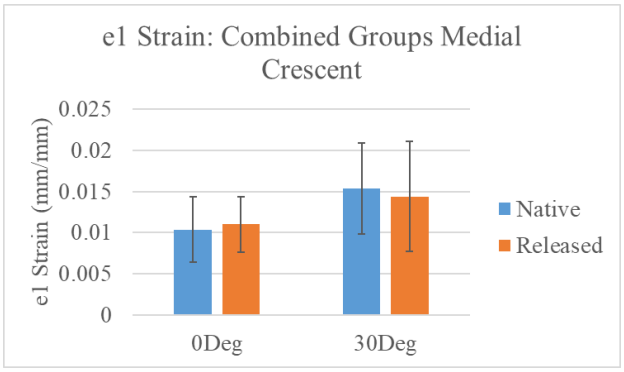

Figure 21. Combined Medial Crescent Strain Results

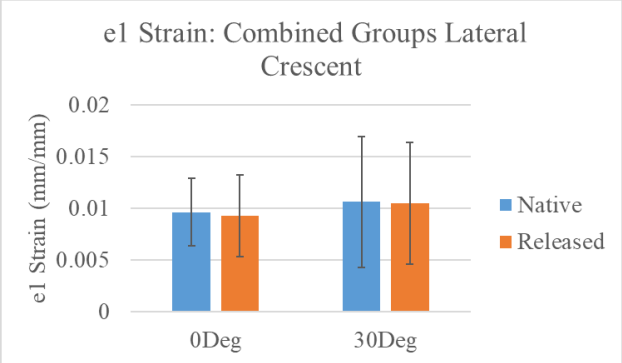

Figure 22. Combined Lateral Crescent Strain Results

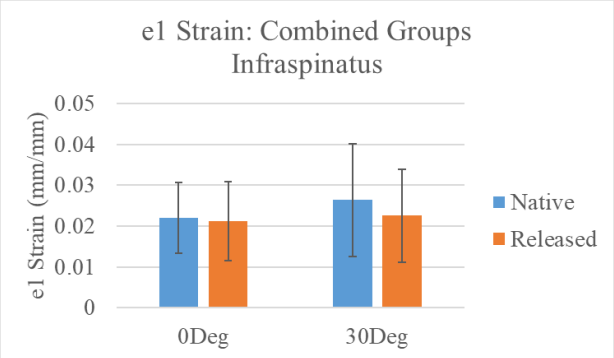

Figure 23. Combined Infraspinatus Strain Results

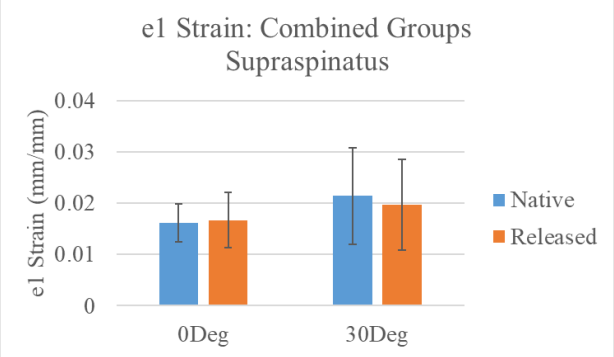

Figure 24. Combined Supraspinatus Strain Results

5.0 Discussion

According to Burkhart's hypothesis, the rotator cable acts as a stress shield for the rotator crescent. This means that as force is applied to the rotator cuff muscles to cause abduction, the rotator cable diverts these forces away from the rotator crescent by bearing the load itself. Based on this hypothesis, it can be concluded that releasing the cable from its intact state should show some significant increase in strain or decrease in abduction force.

Neither the anterior nor posterior groups of the abduction force results showed any significance between release states at 0 or 30 degrees of abduction. This is contrary to Burkhart's hypothesis from which a decrease in abduction force would be expected. Unlike the separated results, the combined abduction force results showed significance at 0 degrees of abduction. This shows that the crescent area where the supraspinatus and infraspinatus insert transmits abduction force from the muscles to the humerus. The main finding that can be concluded about the rotator cable from this is that the crescent area may be a more effective abductor than the cable.

When looking at the anterior and posterior groups separately, the results from this study showed no significant change in major principal strain in the supraspinatus, infraspinatus, or either crescent region. Furthermore, there was little consistency between the regions and release progression groups as to whether the strain increased or decreased in a region with cable release progression. Most of the release progressions fell into one of three categories: the strain decreasing over the progression of the cable release, the strain decreasing only in the single release stage, or the strain decreasing in the single release phase. Similar to the separate anterior and posterior results, the results of the combined analysis for the strain groups showed no significant change. The lack of change in strain in any of the findings of this study is contrary to Burkhart's hypothesis that the cable serves as a stress shield for the rotator crescent.

6.0 Conclusion and Future Work

6.1 Conclusions

The findings of this study suggest that the rotator cable does not function as a stress shield to the rotator crescent region. Therefore, tears in the rotator crescent should be treated as mechanically significant regardless of the rotator cable.

6.2 Future Work

The abduction force increasing significantly at 0 degrees of abduction can likely be explained by the crescent area being a more effective abductor than the cable. However, to draw any further conclusions, further testing should be done to examine exactly why the abduction force increases. Examining the effect releasing the rotator cable has on other shoulder motion aside from abduction might reveal if something is lost from the abduction force that is gained.

Appendix A Abduction Force Data

Table 2. Anterior Specimen Abduction Force Data

Specimen #	Intact (N)		Partial Release (N)		Full Release (N)	
	0°	30°	0°	30°	0°	30°
1	19.84	7.40	31.42	8.04	32.13	8.70
2	8.51	4.10	23.65	4.62	23.30	7.51
3	18.52	4.75	17.02	4.16	22.33	4.28
4	16.06	8.54	24.08	10.93	27.57	10.30

Table 3. Posterior Specimen Abduction Force Data

Specimen #	Intact (N)		Partial Release (N)		Full Release (N)	
	0°	30°	0°	30°	0°	30°
5	19.11	6.72	21.95	6.61	23.76	9.75
6	5.58	3.17	5.76	4.46	4.67	4.54
7	9.28	5.67	11.61	5.30	12.71	4.24
8	21.38	6.41	25.96	6.77	27.87	6.31

Appendix B Major Principal Strain Data

Table 4. Anterior Specimen Medial Crescent Major Principal Strain Data

Specimen #	Intact		Partial Release		Full Release	
	0°	30°	0°	30°	0°	30°
1	1.53E-02	2.00E-02	2.26E-02	1.45E-02	1.46E-02	1.10E-02
2	4.88E-03	1.52E-02	4.61E-03	2.66E-02	7.45E-03	2.34E-02
3	9.68E-03	1.16E-02	1.44E-02	7.99E-03	1.24E-02	9.79E-03
4	1.47E-02	2.07E-02	1.90E-02	1.72E-02	1.55E-02	1.51E-02

Table 5. Posterior Specimen Medial Crescent Major Principal Strain Data

Specimen #	Intact		Partial Release		Full Release	
	0°	30°	0°	30°	0°	30°
5	8.58E-03	1.15E-02	8.53E-03	6.16E-03	8.62E-03	1.09E-02
6	5.75E-03	6.91E-03	7.19E-03	6.02E-03	6.19E-03	5.04E-03
7	1.37E-02	2.33E-02	1.24E-02	2.46E-02	1.27E-02	2.42E-02
8	1.04E-02	1.38E-02	8.46E-03	1.56E-02	1.05E-02	1.58E-02

Table 6. Anterior Specimen Lateral Crescent Major Principal Strain Data

Specimen #	Intact		Partial Release		Full Release	
	0°	30°	0°	30°	0°	30°
1	9.27E-03	6.54E-03	1.77E-02	3.51E-03	8.10E-03	7.47E-03
2	6.04E-03	6.27E-03	2.27E-03	8.47E-03	3.68E-03	1.05E-02
3	7.37E-03	3.04E-03	8.07E-03	2.30E-03	7.90E-03	2.36E-03
4	1.48E-02	1.86E-02	1.81E-02	1.47E-02	1.35E-02	1.48E-02

Table 7. Posterior Specimen Lateral Crescent Major Principal Strain Data

Specimen #	Intact		Partial Release		Full Release	
	0°	30°	0°	30°	0°	30°
5	8.76E-03	9.67E-03	7.93E-03	5.21E-03	7.47E-03	9.53E-03
6	6.05E-03	5.52E-03	7.90E-03	5.26E-03	6.40E-03	3.78E-03
7	1.15E-02	1.73E-02	1.11E-02	1.77E-02	1.16E-02	1.78E-02
8	1.31E-02	1.79E-02	1.23E-02	1.80E-02	1.56E-02	1.76E-02

Table 8. Anterior Specimen Infraspinatus Major Principal Strain Data

Specimen #	Intact		Partial Release		Full Release	
	0°	30°	0°	30°	0°	30°
1	2.25E-02	2.50E-02	3.85E-02	1.81E-02	1.13E-02	6.23E-03
2	1.81E-02	6.97E-03	2.68E-02	1.22E-02	3.37E-02	9.99E-03
3	7.26E-03	1.25E-02	1.16E-02	1.41E-02	9.87E-03	2.13E-02
4	2.47E-02	3.07E-02	2.69E-02	1.84E-02	2.30E-02	2.13E-02

Table 9. Posterior Specimen Infraspinatus Major Principal Strain Data

Specimen #	Intact		Partial Release		Full Release	
	0°	30°	0°	30°	0°	30°
5	3.46E-02	4.73E-02	5.31E-02	5.84E-02	2.23E-02	3.85E-02
6	2.04E-02	1.61E-02	1.58E-02	1.62E-02	1.46E-02	2.23E-02
7	1.71E-02	3.75E-02	1.72E-02	2.54E-02	1.92E-02	2.38E-02
8	3.20E-02	3.53E-02	2.99E-02	2.73E-02	3.58E-02	3.74E-02

Table 10. Anterior Specimen Supraspinatus Major Principal Strain Data

Specimen #	Intact		Partial Release		Full Release	
	0°	30°	0°	30°	0°	30°
1	8.14E-03	3.25E-02	1.04E-02	2.21E-02	1.20E-02	9.68E-03
2	1.51E-02	1.16E-02	3.00E-02	1.25E-02	2.52E-02	1.54E-02
3	1.81E-02	1.56E-02	1.98E-02	1.20E-02	1.74E-02	1.36E-02
4	1.65E-02	2.03E-02	1.05E-02	1.96E-02	1.26E-02	2.09E-02

Table 11. Posterior Specimen Supraspinatus Major Principal Strain Data

Specimen #	Intact		Partial Release		Full Release	
	0°	30°	0°	30°	0°	30°
5	1.77E-02	3.48E-02	1.53E-02	1.74E-02	1.48E-02	3.57E-02
6	1.49E-02	1.10E-02	1.73E-02	1.32E-02	1.36E-02	1.28E-02
7	2.06E-02	1.70E-02	1.46E-02	1.76E-02	1.31E-02	2.07E-02
8	1.78E-02	2.86E-02	1.51E-02	2.05E-02	2.47E-02	2.91E-02

Bibliography

1. Burkhart S. S., Esch J. C., & Jolson R. S. (1993). The rotator crescent and rotator cable: an anatomic description of the shoulder's "suspension bridge". *Arthroscopy*, *9*(6), 611–616.
2. Kim, H. M., et al. (2010). Location and initiation of degenerative rotator cuff tears: an analysis of three hundred and sixty shoulders. *The Journal of Bone and Joint Surgery. American Volume*, *92*(5), 1088–1096.
3. Clark, J. M., & Harryman, D. T., 2nd (1992). Tendons, ligaments, and capsule of the rotator cuff. Gross and microscopic anatomy. *The Journal of Bone and Joint Surgery. American Volume*, *74*(5), 713–725.
4. Ishihara, Y., et al. (2014). Role of the superior shoulder capsule in passive stability of the glenohumeral joint. *Journal of Shoulder and Elbow Surgery, 23*(5): 642-648.
5. Mihata, T., et al. (2013). "Clinical results of arthroscopic superior capsule reconstruction for irreparable rotator cuff tears." *Arthroscopy: The Journal of Arthroscopic & Related Surgery*, *29*(3), 459-470.
6. Renström P., Arms S. W., Stanwyck T. S., Johnson R. J., & Pope M. H. (1986). Strain within the anterior cruciate ligament during hamstring and quadriceps activity. *The American Journal of Sports Medicine*, *14*(1), 83–87.
7. Reilly, P., Amis, A. A., Wallace, A. L., & Emery, R. J. H. (2003). Mechanical factors in the initiation and propagation of tears of the rotator cuff: quantification of strains of the supraspinatus tendon in vitro. *Journal of Bone and Joint Surgery. British volume*, *85*(4), 594-599.

8. Mazzocca, A. D., et al. (2008). Intra-articular partial-thickness rotator cuff tears: analysis of injured and repaired strain behavior. *The American Journal of Sports Medicine, 36*(1), 110-116.
9. Andarawis-Puri, N, Ricchetti, E. T., & Soslowsky, L. J. (2009). Rotator cuff tendon strain correlates with tear propagation. *Journal of Biomechanics, 42*(2), 158-163.
10. Bey, M. J., Song, H. K., Wehrli, F. W., & Soslowsky, L. J. (2002). Intratendinous strain fields of the intact supraspinatus tendon: the effect of glenohumeral joint position and tendon region. *Journal of Orthopaedic Research*, *20*(4), 869–874.
11. Miller, R. M., Fujimaki, Y., Araki, D., Musahl, V. & Debski, R. E. (2014). Strain distribution due to propagation of tears in the anterior supraspinatus tendon. *Journal of Orthopaedic Research, 32*, 1283-1289.
12. Miller R. M., Thunes J., Musahl V., Maiti S., Debski R. E. (2018). Effects of tear size and location on predictions of supraspinatus tear propagation. *Journal of Biomechanics, 68*, 51–57.
13. Pinkowsky, G. J., et al. (2017). Partial-thickness tears involving the rotator cable lead to abnormal glenohumeral kinematics. *Journal of Shoulder and Elbow Surgery*, *26*(7), 1152-1158.
14. Mesiha, M. M., Derwin, K. A., Sibole, S. C., Erdemir, A., McCarron, J. A. (2013). The biomechanical relevance of anterior rotator cuff cable tears in a cadaveric shoulder model. *Journal of Bone and Joint Surgery*, *95*(20), 1817-1824.
15. Kedgley, A. E., et al. (2007). The effect of muscle loading on the kinematics of in vitro glenohumeral abduction. *Journal of Biomechanics*, *40*(13), 2953-2960.

16. Parsons, I. M., Apreleva, M., Fu, F. H., & Woo, S. L. (2002). The effect of rotator cuff tears on reaction forces at the glenohumeral joint. *Journal of Orthopaedic Research*, *20*(3), 439–446.
17. Omi, R., et al. (2010). Function of the shoulder muscles during arm elevation: an assessment using positron emission tomography. *Journal of Anatomy*, *216*(5), 643–649.